Fabrication of a Solution-Processed IGZO/NiO P-N Diode

Nima Arjmandi[*1], Mohammad Seraj[2]

[1] Shahid Beheshti University of Medical Sciences, Velenjak, Tehran, Iran
Nima@Arjmandi.org
+98-9121797552

[2] Islamic Azad University Science and Research Branch, Hesarak, Tehran, Iran
seraj.amn@gmail.com
+98-9338178451

Abstract

The fabrication of a p-n diode is investigated using a fully solution-processed method. Indium gallium zinc oxide (IGZO) ink was synthesized and deposited on a quartz substrate and annealed to form a thin film serving as an n-type semiconductor. A facile sol-gel method was used to deposit a lithium doped nickel oxide thin film (Li:NiO) as a p-type semiconductor. X-ray diffraction (XRD) and scanning electron microscopy (SEM) were employed to characterize the structural properties of Li:NiO and IGZO films. XRD analysis revealed a polycrystalline bunsenite structure in the Li:NiO films. Nanocrystalline grains were also observed on the surface morphology of the Li:NiO films. The XRD analysis indicated that the IGZO films were amorphous. However, SEM images demonstrate a variety of nanostructures in these films, including hexagons. The Li:NiO molar ratio was optimized to minimize series resistance of the diode. NiO had a carrier density of 7.8E13 cm^{-3} and mobility of 0.8 $cm^{-2}/V.S$, the highest mobility ever reported in a NiO film to our knowledge. The carrier density of IGZO was 2.5E16 cm^{-3},and its mobility was 0.95 $cm^{-2}/V.S$. The fabricated diode exhibited a current ratio of 175 in on and off states and a reverse breakdown voltage of 3.5 V

Keywords: printed diode, semiconductor ink, solution process, printed electronics, diode

1. Introduction

Printed electronics is a novel and innovative industry that enables the rapid prototyping of electronic products at a low cost. Additionally, as an additive manufacturing processes, it reduces material consumption and demonstrate a lesser environmental impact. Electronic materials are deposited in this technology via inkjet, screenprint, offset, gravure, or electrostatic printing, typically using liquid inks [1-10]

Various essential devices such as thin-film transistors [11], capacitors [12], resistors [13], and diodes are fabricated using printed electronics. However, many of these devices are not fully printed or solution-processed yet, and vacuum processes are used at some point during their fabrication[14-16], despite the primary reason for the cost savings in this technology being the elimination of vacuum processes.

Among the printable semiconductor materials available, indium–gallium–zinc–oxide (IGZO) exhibits an attractive commercial potential due to its high electron mobility, visible light transparency, and reliability [17, 18]. Furthermore, amorphous indium gallium zinc oxide (a-IGZO) is a robust semiconductor material used as the active layer in oxide thin-film transistors (TFTs). Moreover, the amorphous nature of a-IGZO films enables uniform synthesis over a large area, and their low processing temperature enables their use in flexible devices [19, 20].

Nickel oxide (NiO) has garnered considerable interest for applications such as electrochromic films [21], gas sensors [22], fuel cells [23], the anode of organic light-emitting diodes [24], and thermoelectric materials [25], owing to its p-type conductivity, wide bandgap ranging from 3.6 eV to 4.0 eV, excellent chemical stability, electrical, and optical properties [26, 27]. NiO stoichiometric is an insulator with a resistivity of $10^{13}\,\Omega\cdot m$ at room temperature. As a result, increasing the electrical conductivity of NiO films is critical for increasing the material's applicability as a p-type material in p-n junctions [28, 29]. In general, the resistivity of NiO films can be decreased by increasing the concentration of Ni^{2+} vacancies during air annealing or by doping with a monovalent atom such as Li or Al [30].

Numerous methods for fabricating diodes in printed or flexible electronics have been previously investigated. Lilja et al. fabricated a metal-insulator-metal (MIM) diode using a straightforward process that began with a wet-etched Cu pattern on PET and gravure printing of an air-stable amorphous organic hole-transporting semiconductor, poly (triarylamine) (PTAA), and a top electrode made of silver flakes ink. The work functions of Ag and Cu are 4.3 and 4.7 eV, respectively, indicating the possibility of two Schottky contacts with different energy barriers [31].

Münzenrieder et al. used a vacuum sputtering system to deposit thin films of NiO and IGZO to create a p-n junction diode [32]. Their NiO and IGZO films achieved a carrier density of 1.6E17 cm^{-3} and 2.2E19 cm^{-3} and carrier mobility of 0.45 $cm^{-2}/V.S$ and 11.8 $cm^{-2}/V.S$, respectively. The diode was fabricated on a flexible substrate at nearly room temperature.

Li et al. described the fabrication of an ultraviolet photodetector based on a p-n heterojunction using magnetron sputtering vacuum deposition of n-type IGZO and p-type nickel oxide (p-NiO) thin films on indium tin oxide (ITO) glass [30]. They observed that the photodetector's performance is primarily determined by the conductivity of the NiO thin film, which can be varied through the oxygen partial pressure during the deposition of the NiO thin film.

The extremely low solubility of precursors in the carrier solvent poses a problem during the synthesis of IGZO and NiO inks. The present work describes an improved method for synthesizing NiO p-type and IGZO n-type semiconductor inks that utilize citric acid to increase the precursors' solubility in the solvent. Historically, solution-processed high-quality p-type oxide semiconductor films lagged behind n-type films in terms of development. We have demonstrated that solution-processed NiO p-type films exhibit comparable mobility and carrier density to n-type IGZO films based on synthesized inks. To this end, we introduce a low-cost, fully solution-based fabrication process for fabricating p-n diodes which unlike previous works does not require any vacuum process. To our knowledge, this is the first fully solution-processed diode reported.

2. Experimental Section

2.1. IGZO Synthesis

The IGZO ink was prepared by dissolving 0.1 M zinc acetate dehydrate [$Zn(OAc)_2.2H_2O$], 0.1 M indium chloride, and 0.025 M gallium chloride (atom ratio of Ga:In:Zn is 25:100:100) in a 2-methoxyethanol solvent. Then, 0.2 M monoethanolamine (MEA) was added as a stabilizer [33]. A trace amount of citric acid (10% w) is added to the solution to increase the solubility of indium and gallium precursors in the solvent [34]. We have not found any trace of this material in the final IGZO film. This is probably due to the complete decomposition and vanishing of citric acid during the annealing process [35, 36]. Afterward, the solution was stirred for 2 h at 50°C. The solution was then aged for 18 h at 27°C. Finally, the solution was filtered by a 220 nm pore size filter paper. The viscosity and surface tension of the ink were determined to ensure they were within the acceptable range for printing by the material printer DMP-2800 (Fujifilm Dimatix Inc.).

2.2. NiO Synthesis

NiO ink was prepared by dissolving 0.44 M nickel chloride hexahydrate ($NiCl_2.6H_2O$) in butanol. Various concentrations of lithium chloride were dissolved in the solution, including 2, 5, 10, 14, 18, and 20% [37]. After stirring for 2 h, the solution was diluted with citric acid (10% w/v) to obtain a clear and homogeneous green solution. We have not found any trace of this material in the final NiO film. This is probably due to the complete decomposition and vanishing

of citric acid during the annealing process [36, 37]. After 24 h, the solution was filtered through 220 nm pore size filter paper.

2.3. Diode fabrication

Quartz substrates of 10 x 10 mm were cleaned with hot acetone, hot isopropyl alcohol (IPA), deionized (DI) water, followed by nitrogen blow-drying. Then, using a DMP-2800 (Fujifilm Dimatix Inc.), 5 µl of IGZO inkjet was printed on a 9 x 9 mm square on the substrate in several passes (Figure 1). The substrate was then placed in a furnace and heated from room temperature to 300°C within 8 min and remained at this temperature for 10 min. Following that, its temperature ramped to 500℃ within 11 minutes and remained constant for 1 h. Within 2 h, the furnace had gradually cooled to room temperature.

The synthesized NiO ink was printed on a 6 x 6 mm square at the corner of the IGZO square, yielding 5 µl of the ink (Figure 1). Thus, an exposed area of IGZO was evident alongside the exposed area of NiO. The substrate was then placed back in the furnace and heated to 160°C for 10 min. Subsequently, the temperature increased to 390°C within 5 min, remained constant for 1 h, and gradually cooled to room temperature.

Finally, cathode and anode leads were formed by attaching a 30 µm thick silver wire to the exposed regions of the IGZO and NiO films using some silver paste and two wires (Figure 1).

A Dektak surface profiler was used to determine the thickness of IGZO and NiO films and a Bruker D8 X-ray diffractometer (XRD) to evaluate the films' crystallographic structure. SEM (HITACHI S-4800) was employed to examine the surface morphology of the films. The sheet resistance of the films was determined using a four-point probe instrument. The electron and hole mobilities and carrier concentrations were measured using the Hall Effect, Ecopia HMS-3000. We used a Keithley 590 *C-V* analyzer for capacitance-voltage profiling, and a Keithley 4200A-SCS parameter analyzer was used to measure the *I-V* curves. Sheet resistance of the films is measured by a four-point probe system.

3. Results and Discussion

3.1. IGZO Synthesis

Evaporation of the ink's solvent began immediately after the ink droplets were jetted from the inkjet's nozzle head. However, when samples were heated above 71°C, their solvents evaporated. Hydrolysis processes also occurred during the initial bake at 300°C. $GaCl_3$, $InCl_3$, and $Zn(OAc)_2.2H_2O$ were decomposed and hydrolyzed at this temperature to form $Ga(OH)_3$, $In(OH)_3$, and $Zn(OH)_2$, respectively. The chemical reaction was [33]:

$$InCl_3 + GaCl_3 + Zn(CH3COO)_2 + 6H_2O \rightarrow In(OH) + Ga(OH) + Zn(OH) + xCHCOOH(\uparrow) + yHCl(\uparrow)$$
(Equation 1)

During the second bake, when the temperature of the samples was ramped up to 500°C, a minor exothermic reaction occurred, resulting in a slight weight loss [33]. The dihydroxylation reaction of intermediate materials occurred at this stage. Specifically, $Ga(OH)_3$, $In(OH)_3$, and $Zn(OH)_2$ produce IGZO through the following reaction [33]:

$$In(OH)_3 + Ga(OH)_3 + Zn(OH)_2 \rightarrow InGaZnO_x + yH_2O(\uparrow) \quad \text{(Equation 2)}$$

Figure 2 depicts the XRD spectra of the IGZO film. This spectrum is nearly identical to that of the quartz substrate. Other than the single diffraction peak at 22.4° caused by the quartz substrate, no prominent diffraction peaks were observed, indicating that the solution-processed IGZO film's structure is amorphous. This is consistent with the findings of other studies [33, 38].

Figure 3 illustrates a typical secondary electron microscope (SEM) image of the IGZO film. As demonstrated in previous studies [33, 34], these films are composed of nanostructures ranging in size from ~100 nm to ~200 nm.

One of the advantages of IGZO is that its electrical properties can be easily modulated by adjusting the indium-gallium stoichiometric ratio. Increased gallium concentration in IGZO suppresses oxygen vacancy generation and, as a result, the concentration of its majority carrier. This phenomenon has previously been used to reduce the off-state current of IGZO-TFT devices, which is critical for minimizing power consumption [38, 39]. On the other hand, increasing the Ga concentration in these semiconductors may reduce their electron mobility, as there will be insufficient oxygen vacancies and thus free electrons to prefill trap states [39, 40]. The IGZO in the current study exhibited a majority carrier (electron) density of $2.5x10^{+16}\ cm^{-3}$ and Hall mobility of $0.95\,cm^{-2}/V.S$ according to the Hall effect measurements. Its sheet resistance according to the four-point probe measurements is approximately 550 $K\Omega/sq$. These values are comparable to previous reports [41, 42].

3.2. NiO synthesis

The following chemical reaction results in the formation of the NiO film [37]:

$$NiCl_2.6H_2O \rightarrow NiO\downarrow + 2HCl\uparrow + 5H_2O\uparrow \quad \text{(Equation 3)}$$

However, this pure NiO film's electrical conductance and hole concentration are incredibly low. We doped it with lithium to make it sufficiently p-type and discovered that a 14% molar lithium concentration resulted in the lowest NiO sheet resistance and diode series resistance. The variation in sheet resistance of NiO films as a function of Li concentrations is depicted in Figure 4.

The sheet resistance of the NiO film decreased as the Li doping concentration increased, reaching its minimum value at 14% Li doping concentration. A further increase of the resistance occurs as the Li concentration increases. This corresponds to previous observations and hypotheses [29]. The NiO in the current study exhibited a carrier density of $7.8x10^{+13}\ cm^{-3}$, and the holes in the material demonstrated Hall mobility of $0.8\,cm^{-2}/V.S$ according to the Hall effect measurement.

The NiO films were crystallographically analyzed using a CuKα radiation source with a wavelength of λ=1.54056A°, and their diffraction patterns were recorded by varying the diffraction angle (2θ) from 20° to 80°. The X-ray diffraction patterns of a Li-doped NiO film are shown in Figure 5, it has 20% Li concentration and this NiO film is annealed at 390°C. The Bragg peaks at 37.25, 43.28, 62.9190, and 75.53 were indexed to the (1 1 1), (2 0 0), and (2 2 0) planes, respectively, and the increase in peak intensity may be attributed to either grain growth associated with increased thicknesses or to an increase in crystallinity caused by increasing the solution molarity [29].

Figure 6 depicts SEM images of the Li:NiO thin film. The average grain size is approximately 80 nm. This surface morphology is consistent with that previously described by Raut et al. [37].

3.3. Diode characteristic

Surface profilometer measurements shows final thickness of the IGZO film is about 70 nm ±20 nm and thickness of the NiO film is about 250 nm ±50 nm. The IGZO was printed in 20 passes and the NiO film was printed in 100 passes.

The *I–V* characteristics of the printed diode are depicted in Figure 7. The diodes demonstrated rectifying behavior with an effective threshold voltage ($V_{TH,eff}$) of approximately 0.5 V.

The current ratio between on and off states was approximately 175 ($V = \pm 2$), and the reverse breakdown voltage was approximately 3.5 V.

To measure *C-V* characteristic of the diode, the Keithley 590 *C-V* analyzer applies a 100 kHz sine wave that is superimposed on a DC bias. Considering the dimensions of these diodes, we can only observe high frequency characteristics here. DC bias is started at -2 V and increased to +5 V in a few steps. At each DC bias the measurement system stays for 1 s, then, does the capacitance measurement for 1 s and changes to the next DC bias at 10 V/s. So, here in these measurements the sweep rate is considered slow as well. Considering the relatively small breakdown voltage of these diodes, we could not extend the range of the DC bias. Thus, we

could not use this *C-V* measurement to calculate the carrier concentrations. Figure 8 illustrates the diode's capacitance as a function of the applied voltage. Capacitance increases as forward biasing increases, which is in line with previous studies.

4. Conclusion

In summary, two types of semiconductor inks were synthesized: p-type Li-NiO and n-type IGZO. After printing IGZO and Li-NiO thin films on a quartz substrate, they were annealed at 500°C and 390°C, respectively. The XRD analysis confirmed the amorphous nature of the IGZO. Lithium concentration was optimized in Li-NiO to minimize its sheet resistance. The XRD analysis revealed that the Li:NiO films exhibited a polycrystalline bunsenite structure. Finally, a fully solution-processed diode was printed and characterized using these inks. This study demonstrates the feasibility of fabricating semiconductor devices without using vacuum or lithography, using only standard tools such as inkjet printers and ovens. Further optimization of this process may result in a highly reliable and high-quality fully printed diode.

5. References

[1] Kantola. V, Kulovesi. J, Lahti. L, et al, "1.3 Printed electronics, now and future," *Bit Bang,* vol. 63, pp. 204, 2009.

[2] Kunnari. E, Valkama. J, Keskinen. M, et al, "Environmental evaluation of new technology: printed electronics case study," *Journal of Cleaner Production,* vol. 17, no. 9, pp. 791-799, 2009.

[3] Wojcik. P. J, "Printable organic and inorganic materials for flexible electrochemical devices," Universidade NOVA de Lisboa (Portugal), 2013.

[4] Garlapati. S. K, Divya. M, Breitung. B, et al, "Printed electronics based on inorganic semiconductors: from processes and materials to devices," *Advanced Materials,* vol. 30, no. 40, pp. 1707600, 2018.

[5] Beedasy. V, and Smith. P. J, "Printed electronics as prepared by inkjet printing," *Materials,* vol. 13, no. 3, pp. 704, 2020.

[6] Khan. Y, Thielens. A, Muin. S, et al, "A new frontier of printed electronics: flexible hybrid electronics," *Advanced Materials,* vol. 32, no. 15, pp. 1905279, 2020.

[7] Hamjah. M. K, Steinberger. M, Tam. K. C, et al, "Aerosol jet printed AgNW electrode and PEDOT: PSS layers for organic light-emitting diode devices fabrication." pp. 1-4.

[8] Hooper. W. J, Huebner. W. C, *Electrostatic printing method and apparatus*, U.S, 1951.

[9] Dungchai. W, Chailapakul. O, and Henry. C. S, "A low-cost, simple, and rapid fabrication method for paper-based microfluidics using wax screen-printing," *Analyst,* vol. 136, no. 1, pp. 77-82, 2011.

[10] Suganuma. K, *Introduction to printed electronics*: Springer Science & Business Media, 2014.

[11] Levy. D. H, Scuderi. A. C. and Irving, L.M., et al , *Methods of making thin film transistors comprising zinc-oxide-based semiconductor materials and transistors made thereby*, U.S, 2008.

[12] Cook. B. S, Cooper. J. R, and Tentzeris. M. M, "Multi-layer RF capacitors on flexible substrates utilizing inkjet printed dielectric polymers," *IEEE Microwave and Wireless Components Letters,* vol. 23, no. 7, pp. 353-355, 2013.

[13] Inoue. K, Haruta. Y, Yamanaka. M, et al, "Printed circuit board having electromagnetic wave shield layer and self-contained printed resistor," Google Patents, 1993.
[14] Sani. N, Robertsson. M, Cooper. P, et al, "All-printed diode operating at 1.6 GHz," *Proceedings of the National Academy of Sciences,* vol. 111, no. 33, pp. 11943-11948, 2014.
[15] Odaki. T, Ichikawa. M, Ichikawa. A, et al, "Light-emitting diode device," Google Patents, 2003.
[16] Semple. J, Georgiadou. D. G, Wyatt-Moon. G, et al, "Flexible diodes for radio frequency (RF) electronics: a materials perspective," *Semiconductor Science and Technology,* vol. 32, no. 12, pp. 123002, 2017.
[17] Zhang. J, Li. Y, Zhang. B, et al, "Flexible indium–gallium–zinc–oxide Schottky diode operating beyond 2.45 GHz," *Nature communications,* vol. 6, no. 1, pp. 7561, 2015.
[18] Jo. J. W, Kim. J, Kim. K. T, et al, "Highly stable and imperceptible electronics utilizing photoactivated heterogeneous sol-gel metal–oxide dielectrics and semiconductors," *Advanced Materials,* vol. 27, no. 7, pp. 1182-1188, 2015.
[19] Oh. S.-I, Choi. G, Hwang. H, et al, "Hydrogenated IGZO thin-film transistors using high-pressure hydrogen annealing," *IEEE transactions on electron devices,* vol. 60, no. 8, pp. 2537-2541, 2013.
[20] Wager. J. F, Yeh. B, Hoffman. R. L, et al, "An amorphous oxide semiconductor thin-film transistor route to oxide electronics," *Current Opinion in Solid State and Materials Science,* vol. 18, no. 2, pp. 53-61, 2014.
[21] Purushothaman. K, and Muralidharan. G, "The effect of annealing temperature on the electrochromic properties of nanostructured NiO films," *Solar Energy Materials and Solar Cells,* vol. 93, no. 8, pp. 1195-1201, 2009.
[22] I. Castro-Hurtado, J. Herran, N. Perez, et al, "Toxic gases detection by NiO sputtered thin films," *Sensor letters,* vol. 9, no. 1, pp. 64-68, 2011.
[23] Li. Y, Xie. Y, Gong. J, et al "Preparation of Ni/YSZ materials for SOFC anodes by buffer-solution method," *Materials science and engineering: B,* vol. 86, no. 2, pp. 119-122, 2001.
[24] Kraft. T. M, Berger. P. R, and Lupo. D, "Printed and organic diodes: devices, circuits and applications," *Flexible and Printed Electronics,* vol. 2, no. 3, pp. 033001, 2017.
[25] Shin. W, and Murayama. N, "High performance p-type thermoelectric oxide based on NiO," *Materials Letters,* vol. 45, no. 6, pp. 302-306, 2000.
[26] Ail. A. H, and Kadhim. R. R, "Effect of copper doping on the some physical properties of Nio thin films prepared by chemical spray pyrolysis," *International Journal of Application or Innovation in Engineering & Management,* vol. 4, pp. 2319-4847, 2015.
[27] Jang. W.-L, Lu. Y.-M, Hwang. W.-S., et al, "Electrical properties of Li-doped NiO films," *Journal of the European Ceramic Society,* vol. 30, no. 2, pp. 503-508, 2010.
[28] Nandy. S, Saha. B, Mitra. M. K., et al, "Effect of oxygen partial pressure on the electrical and optical properties of highly (200) oriented p-type Ni 1− x O films by DC sputtering," *Journal of materials science,* vol. 42, pp. 5766-5772, 2007.
[29] Nandy. S, Maiti. U, Ghosh. C, et al, "Enhanced p-type conductivity and band gap narrowing in heavily Al doped NiO thin films deposited by RF magnetron sputtering," *Journal of Physics: Condensed Matter,* vol. 21, no. 11, pp. 115804, 2009.
[30] Li. H, Chen. T, Hu. S, et al, "Highly spectrum-selective ultraviolet photodetector based on p-NiO/n-IGZO thin film heterojunction structure," *Optics express,* vol. 23, no. 21, pp. 27683-27689, 2015.
[31] Lilja. K. E, Bäcklund. T. G, Lupo. D, et al, "Gravure printed organic rectifying diodes operating at high frequencies," *Organic Electronics,* vol. 10, no. 5, pp. 1011-1014, 2009.
[32] Münzenrieder. N, Zysset. C, Petti. L, et al, "Room temperature fabricated flexible NiO/IGZO pn diode under mechanical strain," *Solid-State Electronics,* vol. 87, pp. 17-20, 2013.

[33] Shen. Y, Liu. Z, Wang. X, et al, “Synthesis of IGZO ink and study of ink-jet printed IGZO thin films with different Ga concentrations,” *Solid-State Electronics,* vol. 138, pp. 108-112, 2017.
[34] Arjmandi. N, Seraj. M, Najafi. M, et al, “Inkjet-printed high quality gate oxide for fully printed IGZO transistors,” in IEEE 16th Nanotechnology Materials and Devices Conference (NMDC), , Vancouver, Canada., 2021.
[35] Barbooti. M. M. a. A.-S. D. A, “Thermal decomposition of citric acid,” *Thermochimica Acta,* vol. 98, pp. 119-126, 1986.
[36] Wyrzykowski. D, Hebanowska. E, Nowak-Wiczk. G, et al, “Thermal behaviour of citric acid and isomeric aconitic acids,” *Journal of Thermal Analysis and Calorimetry,* vol. 104, no. 2, pp. 731-735, 2011.
[37] Guo. W, Hui. K.N, “High conductivity nickel oxide thin films by a facile sol–gel method,” *Materials Letters,* vol. 92, pp. 291-295, 2013.
[38] Wang. Y, Sun. X. W, Goh. G. K. L, et al, “Influence of channel layer thickness on the electrical performances of inkjet-printed In-Ga-Zn oxide thin-film transistors,” *IEEE Transactions on Electron Devices,* vol. 58, no. 2, pp. 480-485, 2010.
[39] Kim. M.-S, Hwan Hwang. Y, Kim. S, et al, “Effects of the oxygen vacancy concentration in InGaZnO-based resistance random access memory,” *Applied Physics Letters,* vol. 101, no. 24, pp. 243503, 2012.
[40] Marks. T, and Facchetti. A, *Transparent electronics: from synthesis to applications*: John Wiley & Sons, 2010.
[41] Hennek. J. W, Xia. Y, Everaerts. K, et al, “Reduced contact resistance in inkjet printed high-performance amorphous indium gallium zinc oxide transistors,” *ACS Applied Materials & Interfaces,* vol. 4, no. 3, pp. 1614-1619, 2012.
[42] Guerrero. E, Polednik. A, Ecker. M, et al, “Indium–Gallium–Zinc Oxide Schottky Diodes operating across the glass transition of stimuli-responsive polymers,” *Advanced Electronic Materials,* vol. 6, no. 4, pp. 1901210, 2020.

6. Figure and table captions

7. figures and tables

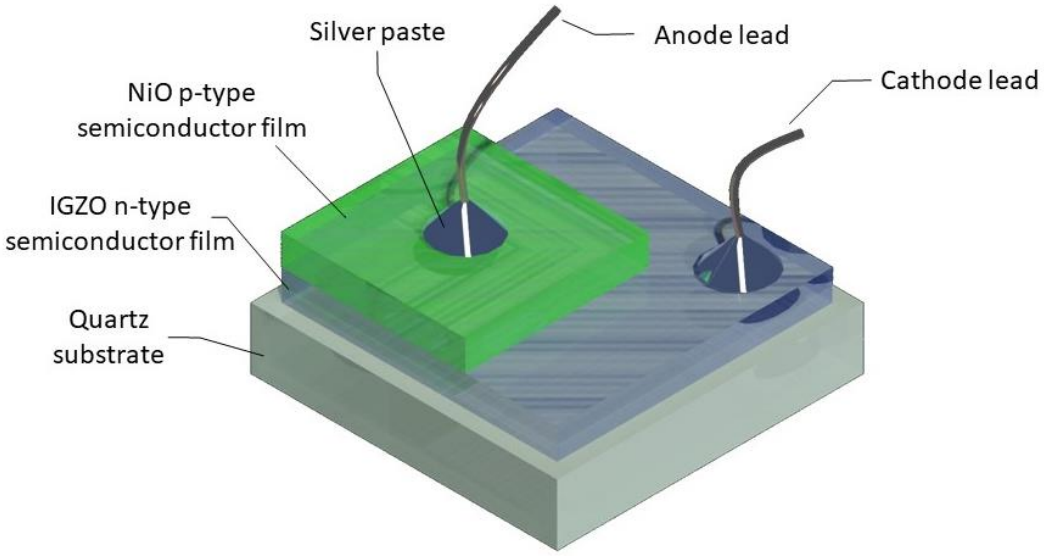

Figure 1. Printed indium gallium zinc oxide (IGZO)/nickel oxide (NiO) diode schematic**.**

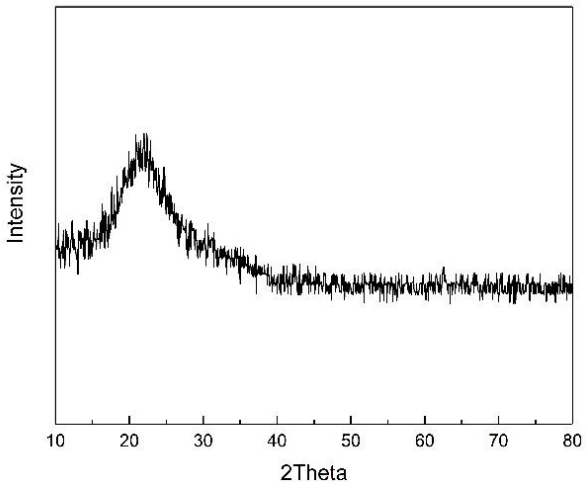

Figure 2. XRD spectra of the IGZO thin film.

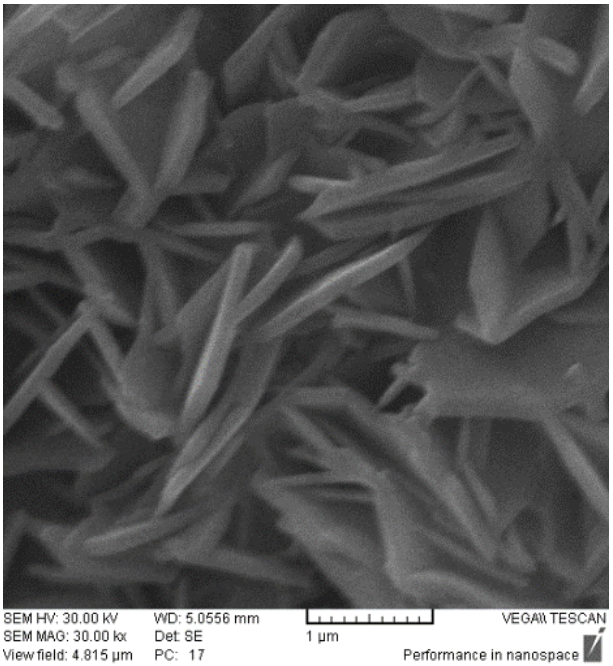

Figure 3. SEM image of the IGZO thin film.

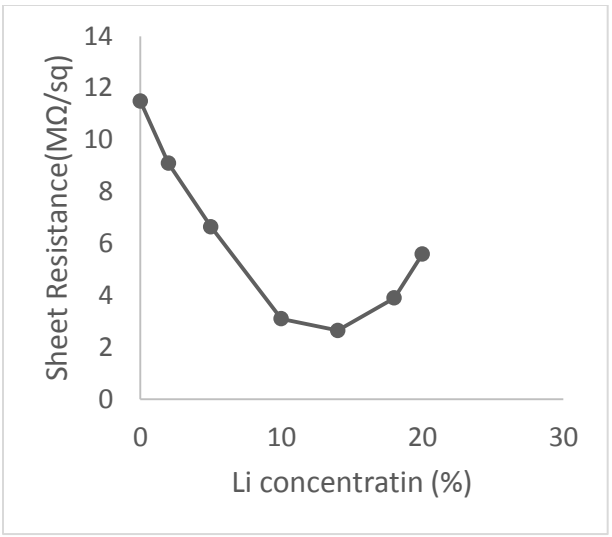

Figure 4. Nickel oxide thin film sheet resistance as a function of Li doping concentration.

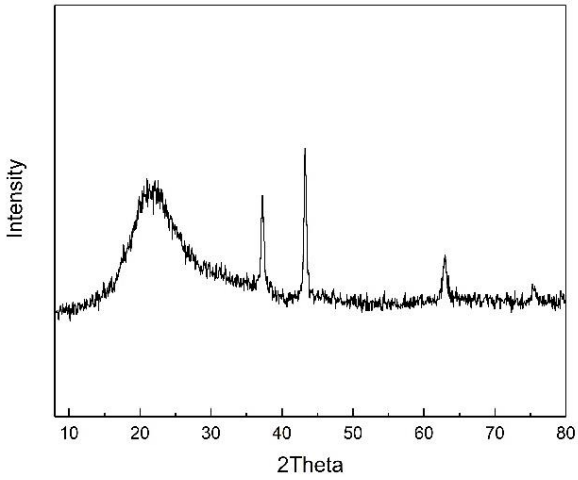

Figure 5. XRD spectra of Li-NiO thin film.

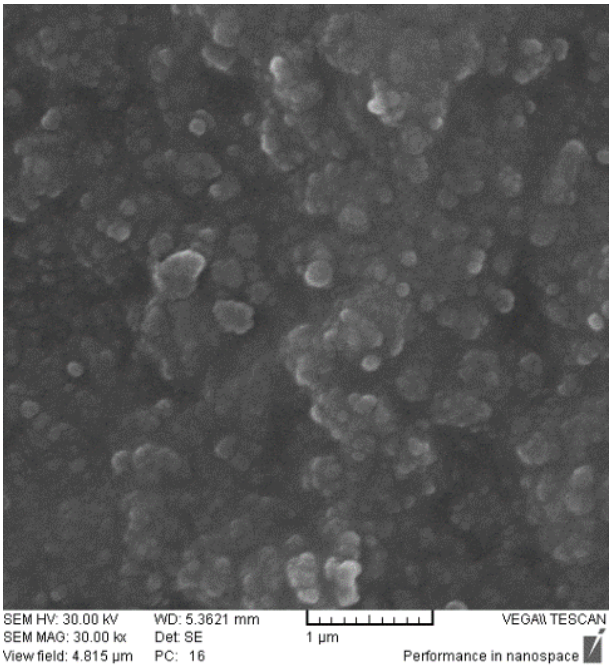

Figure 6. SEM image of the Li:NiO film.

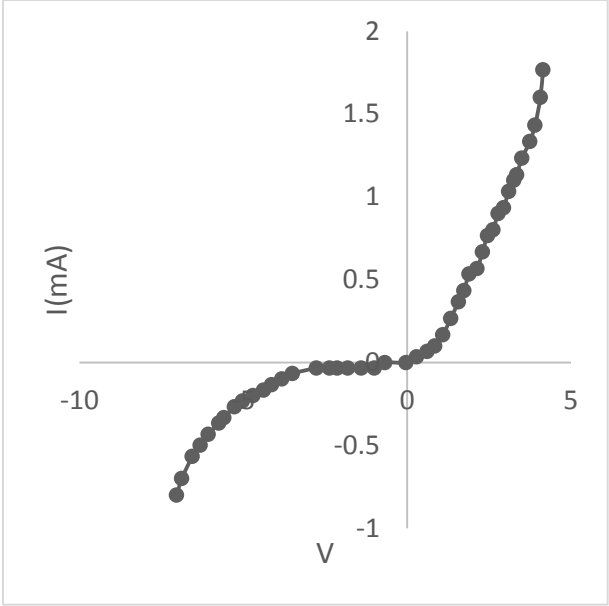

Figure 7. NiO/IGZO diode *I-V* curve.

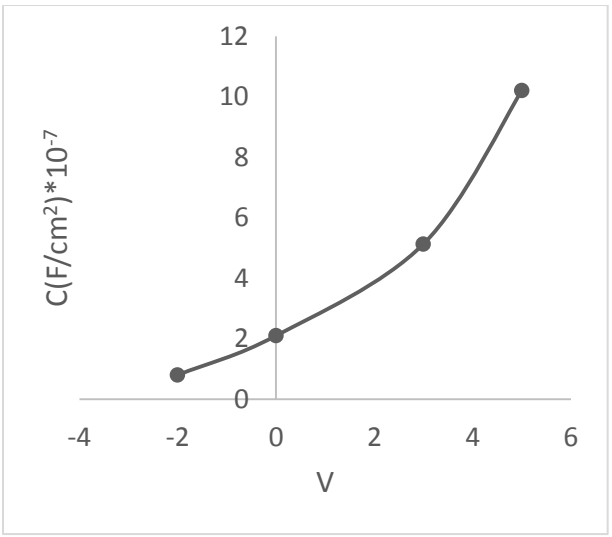

Figure 8. Capacitance variation observed between the diode's cathode and anode as a function of applied voltage.

Biography of Authors

Nima Arjmandi

Ranked 10 amoung about one million students in undergraduate national university entrance exam,

BSc in medical engineering from Shahid Beheshti University of Medical Sciences,

Ranked 1 amoung about 100’000 students in graduate national university entrance exam,

MSc in nanoelectronic device fabrication from Sharif University of Technology,

PhD in nanoelectronic device fabrication from IMEC,

Several years of teaching experience in universities in different countries in the field of advanced electronic devices fabrication; promoter of more than 10 MSc and more than 5 PhD thesises, author of several papers and patents,

Several years of industerial management and development experience in leading edge, mature and legendary semiconductor fabs in different countries,

Manager of several national and international research and development projects,

Manager of several national and international standard development projects.

Mahammad Seraj

BSc in electrical engineering from Islamic Azad University, Sari branch,

MSc in electrical engineering from Islamic Azad University, science and research branch,

A member of a team that for the first time in Iran synthesised semiconductor inks and fabricated the first printed diode and the first printed transistor in Iran,

Participated in several VLSI IC design projects,

Participated in writing the first standard in the field of printed electronics in Iran,

A member of Iran’s TC119 mirror committee in IEC (international electrotechnic committee),

A member of Iran’s young scholars club,

Experienced in designing and building of 3D printing machines.